AIP | Applied Physics Letters

Light induced phase change in Cu2xZn1.3SnS4 thin films

Sunil Kumar Samji, Brajesh Tiwari, M. Krishna Surendra, and M. S. Ramachandra Rao

Citation: Applied Physics Letters **104**, 152106 (2014); doi: 10.1063/1.4871705
View online: http://dx.doi.org/10.1063/1.4871705
View Table of Contents: http://scitation.aip.org/content/aip/journal/apl/104/15?ver=pdfcov
Published by the AIP Publishing

Light induced phase change in $Cu_{2-x}Zn_{1.3}SnS_4$ thin films

Sunil Kumar Samji, Brajesh Tiwari, M. Krishna Surendra, and M. S. Ramachandra Rao[a)]
Department of Physics and Nano Functional Materials Technology Centre, Indian Institute of Technology Madras, Chennai–600036, India

(Received 20 December 2013; accepted 6 April 2014; published online 17 April 2014)

Cu_2ZnSnS_4 and its alloy based thin film solar cells have shown better photovoltaic performance under Cu-poor and Zn-rich conditions. However, the effect of Cu-stoichiometry on the coexistence of kesterite (KS), stannite and/or partially disordered kesterite (PD-KS) phases and their influence on photovoltaic performance is not clearly understood. Raman studies were carried out on $Cu_{2-x}Zn_{1.3}SnS_4$ ($x = 0$, 0.3, and 0.5) thin films by changing the intensity of the incident laser beam. It was observed that both Cu-stoichiometry and incident laser beam intensity induce a disorder in the system. Disorder induced transformation of KS ($I\bar{4}$) to PD-KS ($I\bar{4}2m$) is explained by Raman studies. © *2014 AIP Publishing LLC*. [http://dx.doi.org/10.1063/1.4871705]

Creation of copper vacancies in I-III-VI semiconductors like $CuInX_2$ ($X = S$, Se) lead to the formation of electrically benign grain boundaries (GBs).[1,2] This is the reason why polycrystalline $CuInX_2$ and $Cu(In,Ga)X_2$ based solar cells are more efficient compared to their single crystalline counterparts.[3] There have been reports of some studies on GBs in quaternary semiconductor like Cu_2ZnSnS_4 (CZTS), although this system is not as extensively studied as $CuInX_2$.[4]

Cu-based quaternary semiconductors like CZTS, CZTSe, and CZTSSe are among the category of earth abundant and non-toxic absorber layer materials which form the promising candidates for thin film photovoltaic (PV) market. CZTS has a direct band gap of 1.5 eV and is a p-type semiconductor. So far the most efficient CZTS solar cells are fabricated under Cu-poor and Zn-rich conditions.[5] P-type nature of CZTS is due to native defects involving V_{Cu} (Cu vacancies), Zn_{Cu} and Cu_{Zn} antisite defects.[6,7] For CZTS to reach a matured level of technology and to replace $Cu(In,Ga)Se_2$ (CIGS), there are many fundamental properties which need to be studied and understood. Among the various properties, resolving the ambiguity about the coexistence of kesterite (KS), stannite (ST) and/or partially disordered kesterite (PD-KS) and its effect on photovoltaic performance becomes one of the important objectives of research work on CZTS.

The two forms of CZTS crystal structures namely (i) kesterite ($I\bar{4}$) and (ii) stannite ($I\bar{4}2m$) can be constructed from its ternary counterpart $CuInS_2$ (CIS) structure by replacing 50% of In atoms with that of Zn and the remaining 50% by Sn. CIS has a body centered tetragonal structure, with each anion sitting at the center of the tetrahedron, surrounded by four cations, two Cu and two In atoms (A_2B_2C type tetrahedron). The sum of valence electrons around the center of tetrahedron (contributed by cations) is eight and hence they obey octet rule.[8] While KS structure is obtained from chalcopyrite (CH) structure of CIS, ST structure is obtained from Cu-Au like structure.[9] Both KS and ST structures obey octet rule whereas PD-KS does not obey octet rule.[10] Crystal structures of CIS in chalcopyrite and Cu-Au forms are shown in Figs. 1(a) and 1(b), respectively. Crystal structure of CZTS in KS, ST, and PD-KS forms are shown in Figs. 1(c)–1(e), respectively. In Fig. 1(e), (001) CuZn layer contains spheres with half-blue-half-grey colors, which indicate that the occupation of the particular site by Cu and Zn is equally probable and actual way they arrange is not clear. This random rearrangement of cations in CuZn layer (001) gives rise to a PD-KS structure which has effectively the same symmetry as stannite ($I\bar{4}2m$). Since the way in which the cations are ordered is unknown it is referred to as partially disordered kesterite (PD-KS). KS structure has lower strain energy as well as Madelung energy compared to ST structure and hence possesses low formation energy. Madelung energies of the three structures are KS < ST < PD-KS.[10] KS and ST differ only slightly in the cation arrangement in the sublattice as shown in Figs. 1(c) and 1(d), respectively.[11] Since the difference in the formation energy is very low (3 meV/atom),[9,10] it was expected that both KS and ST phases co-existed in as-synthesized samples.[12]

Structural properties can be studied by X-ray diffraction, neutron diffraction, X-ray synchrotron, and Raman

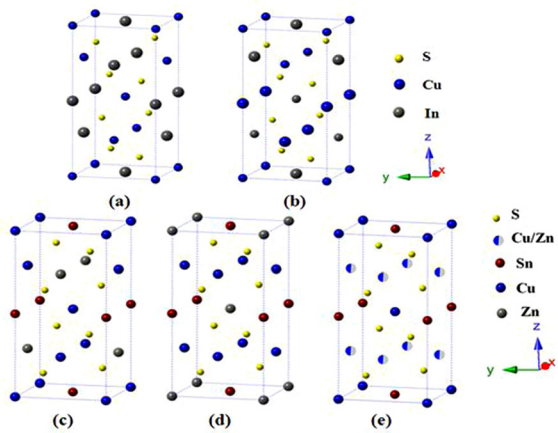

FIG. 1. Representation of crystal structures of (a) CH-$CuInS_2$, (b) Cu-Au $CuInS_2$, (c) KS-CZTS, (d) ST-CZTS, and (e) PD-KS. Directions of different axes are shown. Spheres with different colours are used to indicate different atoms viz. yellow-S, blue-Cu, grey-In and Zn, magenta-Sn and half-blue-half-grey – Cu or Zn.

[a)]Author to whom correspondence should be addressed. Electronic mail: msrrao@iitm.ac.in.

spectroscopy. It is well understood from theoretical as well as experimental studies that X-ray diffraction technique is not sufficient to distinguish KS, ST and/or PD-KS structures.[13,14] Neutron powder diffraction studies by Schorr *et al*. ruled out the presence of ST and indicated the presence of Zn_{Cu} and Cu_{Zn} antisites, which were attributed to PD-KS.[15] Tsukasa *et al*. reported X-ray synchrotron studies on CZTS thin film samples with three different compositions, corresponding to $Cu/(Zn+Sn) = 1.2$, 1.0, and 0.8. They concluded that for $Cu/(Zn+Sn) > 1.0$, Cu tends to occupy Sn site and for $Cu/(Zn+Sn) = 1.0$ and 0.8, Zn substitutes for Cu and/or Cu substitutes for Zn and in the latter case occupancy is relatively more.[16] This work experimentally confirms the presence of Zn_{Cu} and Cu_{Zn} antisite defects in CZTS thin films.

Recently, Valakh *et al*. reported Raman studies on single crystal CZTS at Cu-rich ($Cu/(Zn+Sn) \geq 1.0$) as well as Cu-poor ($Cu/(Zn+Sn) \sim 0.8$) regions[17] and concluded that Cu-rich regions in single crystal are dominated by a narrow peak (FWHM of $4\,cm^{-1}$) at $337\,cm^{-1}$ while the Cu-poor regions are dominated by relatively broader peak at $331\,cm^{-1}$. It was supposed (assumed) that it requires less than 3 meV/atom to transform KS to PD-KS and this may be a first step towards the transformation of KS to ST. Such a supposed transformation from KS to ST through PD-KS is not convincing in the light of the above discussions on Madelung energy and octet rule. It was also reported that, when excited with intensities I_0 and $4I_0$ Raman spectra looked similar to that of Raman spectra on Cu rich and Cu-poor regions, respectively. This was attributed to optical band to band excitation. In order to understand this clearly, Raman studies were carried out on nano-ink based CZTS thin films which differ in their copper stoichiometry.

CZTS thin films can be prepared by various techniques,[18] among them chemical routes have promised efficient and inexpensive solar cell technology compared to PVD techniques. Todorov *et al*. reported an efficiency of 11.1%, which employs hydrazine based sol-gel technique.[5] Guo *et al*. reported an efficiency of 7.2% with nano-ink based solar cells.[19] Stoichiometric ($Zn/Sn = 1$) as well as Cu-poor and Zn-rich CZTS thin films with nominal composition $Cu_{2-x}Zn_{1.3}SnS_4$ ($x = 0$, 0.3, and 0.5) were prepared using hydrazine free nano-ink by drop casting it on a glass substrate and heating it at 350 °C for 1 h in N_2 atmosphere. High pure copper (II) acetate monohydrate (Sigma Aldrich), zinc acetate (Alfa Aeser), tin chloride penta hydrate (Sigma Aldrich), and elemental sulphur (Sigma Aldrich) dissolved in oleylamine (Sigma Aldrich) were used as precursors for the synthesis of nano-ink. In the present work, CZTS nano-ink was prepared from hot-injection technique.[19,20]

Composition was determined from energy dispersive spectroscopy collected by areal EDS using field emission scanning electron microscope (FESEM) (Quanta 3D, FEI, Netherlands) system. $Cu/(Zn+Sn)$ ratios for $x = 0$, 0.3, and 0.5 in $Cu_{2-x}Zn_{1.3}SnS_4$ are 0.95, 0.69, and 0.54, respectively. AFM images of scan size $1\,\mu m \times 1\,\mu m$ were recorded by Bruker dimension edge scanning probe microscope in tapping mode to determine the average particle size. Raman spectra were recorded using Horiba Jobin Yvon spectrometer in the back scattering configuration in the range $100–600\,cm^{-1}$ with an excitation wavelength $\lambda_{exc} = 632.8$ nm of He-Ne laser. The Raman scattered signal was guided to a Peltier-cooled CCD (DV420 A-OE-324) detector. A grating with 1800 grooves/mm with spectral resolution $1\,cm^{-1}$ was used. The intensity of the incident laser beam, acquisition, and accumulation times were carefully adjusted by trial and error basis in order not to damage the samples, since laser annealing is one of the well-known problems in Cu-based chalcopyrites.[21–23] Neutral density filters were used to reduce the intensity of incident laser beam. The factor by which the intensity is reduced is given by equation $I_x = \frac{I_{inc}}{10^x}$ where, I_x is the intensity of the laser beam after using the filter x. I_{inc} is the intensity of the incident laser beam. $x = 2$, 1, and 0.6 and corresponding intensities are designated as I_0, $10I_0$, and $25I_0$, respectively.

Figures 2(a)–2(c) show Raman spectra of $Cu_{2-x}Zn_{1.3}SnS_4$ thin films corresponding to $x = 0$, 0.3, and 0.5, respectively. The most intense A_1 Raman mode appears at $338 \pm 1\,cm^{-1}$ referred to as 339 peak hereafter and the disorder Raman mode appears at $330 \pm 2\,cm^{-1}$ referred to as 331 peak hereafter. Peak positions and their corresponding modes for $Cu_{2-x}Zn_{1.3}SnS_4$ ($x = 0$) along with traceable secondary phases are listed in Table I. Here, the discussion is confined to variation of the intensity ratio I_{339}/I_{331}. The ratio I_{339}/I_{331} is plotted as function of x (Cu deficiency) and intensity of the incident laser beam to understand the effect of both on the presence of PD-KS phase. A solid line is shown in Fig. 2 as a guide to the eye; it can be observed that the peak position of the most intense A_1 phonon mode does not change appreciably with copper deficiency. Khare *et al*. also reported that there is no appreciable Raman shift in the A_1 phonon mode either by changing stoichiometry or cation composition.[13] From Fig. 2(a), it can be observed that a shoulder peak appears around $331\,cm^{-1}$ along with the most intense peak at $339\,cm^{-1}$. The A_1 mode for each composition is expanded and shown as inset in Figs. 2(a)–2(c). In order to identify the effect of copper stoichiometry on the

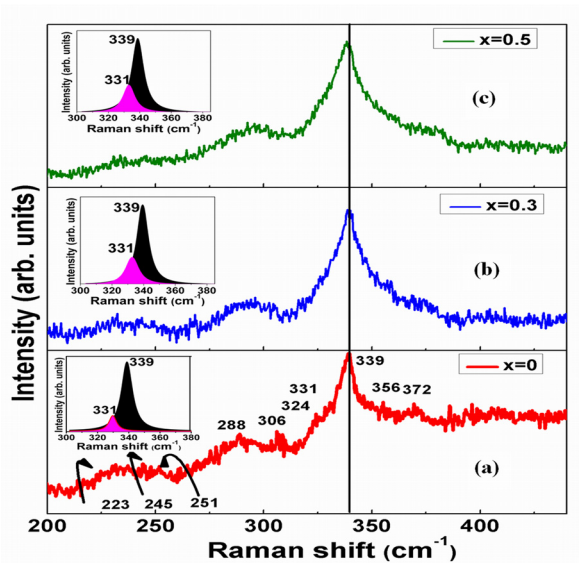

FIG. 2. Raman spectra of $Cu_{2-x}Zn_{1.3}SnS_4$ thin films corresponding to different copper deficiency (a) $x = 0$, (b) $x = 0.3$, and (c) $x = 0.5$. Peak positions of different modes are marked for $x = 0.0$ sample. A line is drawn as a guide to the eye at $339\,cm^{-1}$. The insets show the A_1 mode and disorder phonon mode.

TABLE I. Raman peaks observed in $Cu_{2-x}Zn_{1.3}SnS_4(x=0)$ with corresponding symmetries are tabulated. Peaks of secondary phases are also listed.

Peak position (cm^{-1})	Symmetry/phase
166	B
190	SnS
215	SnS_2
244	E/B (TO)
251	B (LO)
256	E(LO)
264	$Cu_{2-x}S$
275	ZnS
278	E(TO)
289	A
307	Sn_2S_3
316	SnS_2
324	Cu_4SnS_4
331	PD-KS
334	Cu_2SnS_3
339	A_1
341	E
346	E
349	B
351	B
356	ZnS
372	quasi resonant mode

relative intensities of these peaks, the curves were fitted to Lorentzian as shown in the inset of Figs. 2(a)–2(c). It can be observed that the intensity of the 331 peak, corresponding to disorder phonon mode increases relatively and the ratio I_{339}/I_{331} decreases with increasing x (copper vacancies or defects).

One of the possible reasons for peak broadening in Raman spectra on nanomaterials could be due to phonon confinement which is a strong function of particle size. The particle size in the present work was observed to increase with increase in Cu deficiency (x). AFM images and the corresponding histograms clearly show particle size distribution (30–65 nm) and the average particle size calculated from the AFM images are shown in the Figs. 3(a)–3(e), for the three compositions. The average particle sizes are 32 nm, 55 nm, and 66 nm for $x=0$, $x=0.3$ and 0.5, respectively in $Cu_{2-x}Zn_{1.3}SnS_4$. Liu *et al.* reported phonon confinement studies in CZTS nano crystals from which they concluded that confinement in CZTS is only possible in the particle size range 2–10 nm.[24] Moreover, confinement effects are more pronounced when the particle size is comparable to that of Bohr radius, which is around 2.5–3.4 nm for CZTS. However, the particle size in the present work does not fall in this range and hence the asymmetry due to phonon confinement is ruled out.

Though nominally copper deficient CZTS films are prepared, it is not just copper vacancies alone that are created, as theoretical and experimental studies show evidence for the possible creation of other types of defects. Chen *et al.* reported the presence of $Zn_{Cu}+V_{cu}$ under Cu-poor and Zn-rich conditions. Also they reported the presence of compensating defect complex $[Cu^{-}_{Zn}+Zn^{+}_{Cu}]^{0}$, which leads to disorder in the cation sublattice.[6,25] Neutron diffraction studies by Schorr *et al.*[26] and photoluminescence studies by Grossberg *et al.* support the argument.[25] In the present work, broadening of the peak at 339 cm^{-1} has different origin and is not a manifestation of the particle size/phonon confinement. With increase in Cu deficiency, the cost to create such neutral defects reduces, the defect density increases and hence the peak broadens with increase in intensity of the peak at 331 cm^{-1}, which is attributed to PD-KS.[6,27]

If the disorder introduced in the lattice depends on copper deficiency, then it could also be possible that disorder can be introduced by other means. Does the ratio I_{339}/I_{331} decrease in that case? In order to understand this, Raman studies were carried out by exciting the system at three different incident laser beam intensities I_0, I_1 ($10I_0$), and I_2 ($25I_0$). Different peaks in the range 300–380 cm^{-1} for all the three compositions at three different excitation intensities are marked. Peaks at 311 cm^{-1} belongs to Sn_2S_3, 318 cm^{-1} and 348 cm^{-1} to O-Cu_3SnS_4, 322 ± 2 cm^{-1} to Cu_4SnS_4 and 364 cm^{-1} to CZTS, respectively which are well reported.[14,28,29] Of course there are also other peaks which

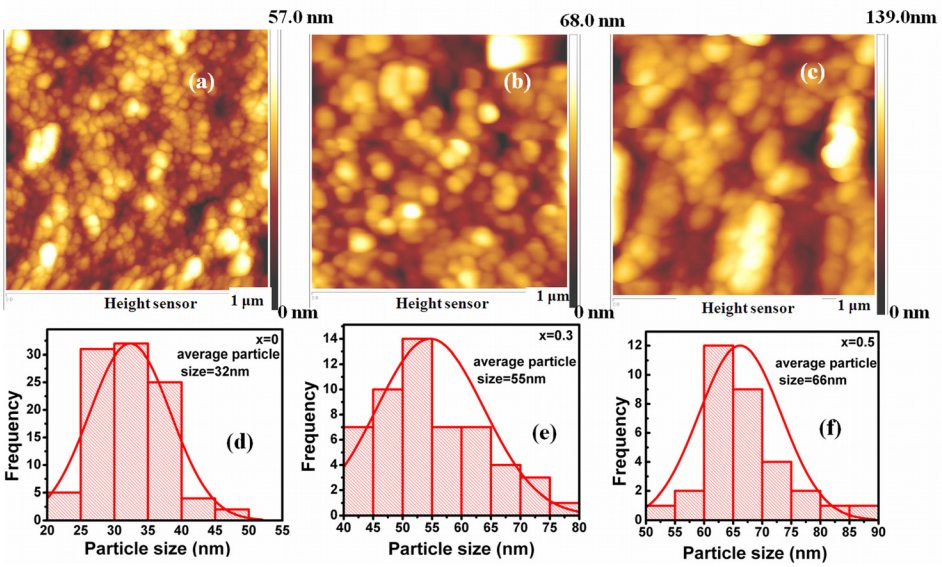

FIG. 3. AFM images of $Cu_{2-x}Zn_{1.3}SnS_4$ thin films recorded for (a) $x=0$, (b) $x=0.3$, and (c) $x=0.5$ compositions. (d), (e), and (f) show corresponding histograms and average particle sizes determined from the histograms.

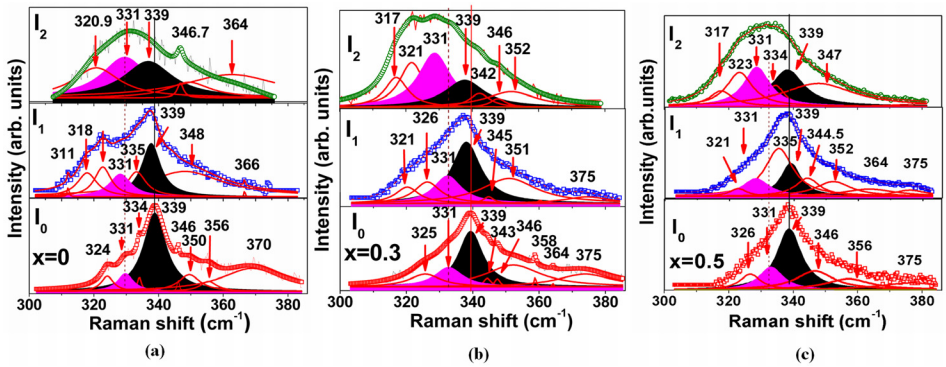

FIG. 4. Raman spectra of $Cu_{2-x}Zn_{1.3}SnS_4$ thin films recorded at three different intensities of incident laser beam I_0, I_1 (10 I_0) and I_2 (25 I_0) corresponding to different Cu-content, (a) x = 0, (b) x = 0.3, and (c) x = 0.5. Intensities of incident laser beam are marked in the graph. The peaks at 331 cm^{-1} and 339 cm^{-1} are given different colour shades to clearly distinguish changes in intensity of the modes with Cu stoichiometry and incident laser beam intensity.

are not mentioned in the Table I. However, these are same as the peaks in Table I shifted few cm^{-1} away from the regular position, e.g., 342 cm^{-1}, 345 cm^{-1}, 350 cm^{-1}, 352 cm^{-1} peaks. It can be observed that the peak at 331 cm^{-1} becomes intense and grows with increasing incident laser beam intensity and this can be observed in a pronounced manner in all the three samples for different Cu-stoichiometries x = 0, 0.3, and 0.5 as shown in Figs. 4(a)–4(c), respectively. The peaks at 339 cm^{-1} and 331 cm^{-1} are given different colour shades to clearly distinguish the change in the ratio I_{339}/I_{331} with the exciting laser beam intensity.

The ratio I_{339}/I_{331} as a function of incident laser beam intensity for different copper stoichiometries is shown in Fig. 5(a). It can be observed that for a given composition (x), as laser beam intensity is increased, the ratio has been found to decrease and for a given laser beam intensity as Cu deficiency increases, the ratio I_{339}/I_{331} has been found to decrease. This is very important and it provides a straight forward evidence of the laser induced disorder in KS $(I\bar{4})$ system mediated by formation of defects leading to the formation of PD-KS structure with effectively the same symmetry as ST $(I\bar{4}2m)$ structure. Disorder is introduced by the creation of defects (Cu deficiency) and/or by laser irradiation which drives the system from a state of lower symmetry $(I\bar{4})$ to higher symmetry $(I\bar{4}2m)$. This is in accordance with the general phenomenon that a system becomes more symmetric with increase in disorder.[30]

The observed change in the relative peak intensities for the peaks at 339 cm^{-1} (KS) and 331 cm^{-1} (PD-KS) with copper stoichiometry and incident laser beam intensity, as shown in Fig. 5(a), can be explained by considering the coexistence of both the structures of CZTS. The coexistence of both the phases can be represented by free energy which consists of two minima as shown in Fig. 5(b). The KS $(I\bar{4})$ is more stable compared to PD-KS $(I\bar{4}2m)$ as marked in Fig. 5(b). The

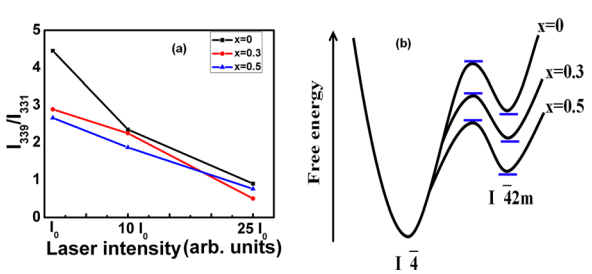

FIG. 5. (a) Variation of ratio I_{339}/I_{331} with the intensity of incident laser beam for different values of x and (b) free energy of two phases KS $(I\bar{4})$ and PD-KS $(I\bar{4}2m)$.

transformation of KS to PD-KS can be achieved in many ways, here it is done by varying copper stoichiometry (x = 0, 0.3, and 0.5) which in turn increases the disorder. This can be understood by invoking reduction in free energy of the disordered system as shown in Fig. 5(b). Increase in incident laser beam intensity also introduces disorder in the cation sublattice, which is equivalent to PD-KS $(I\bar{4}2m)$ structure and hence the decrease in the intensity ratio (I_{339}/I_{331}) is apparent. The difference between a bulk crystal and nanocrystalline thin film is that in the latter case laser heating is more localized due to reduced thermal conductivity and hence relatively more disorder could be possible in nanocrystalline films.[31] Transformation of KS to PD-KS is a disorder induced transformation and is nothing to do with optical band to band excitation (under laser illumination). In fact, it is intrinsic to material property that, in covalently bonded polar semiconductors like $CuInX_2$(X = S, Se), in general a thermodynamically favorable rearrangement of structure by reconstruction of defects happen by creation of row of Cu vacancies to obtain charge neutrality by nullifying the charge created by the formation of polar surfaces. In case of CZTS, it happens by the formation of $[Cu^{-}_{Zn} + Zn^{+}_{Cu}]^0$ neutral defect complex.

It is well known that in selenides, Cu vacancies over large range exhibit no disorder, rather form ordered vacancy compounds (OVCs) and this is well understood by both theoretical and experimental studies in selenides, while the studies are scarcer for sulphides (even for ternary compounds).[32,33] Klein *et al.* reported that in $CuInS_2$ and $CuGaS_2$ OVCs are not formed, in contrary to selenides. Hence, it is too early to comment on the formation of OVCs in quaternary sulphides. Zhang *et al.* reported that in $CuInSe_2$, m (m = 1) units of $[2V_{Cu}^{-} + In_{Cu}^{2+}]$ defect pair repeat over n units of $CuInSe_2$ to form different types of OVCs like $CuIn_5Se_8$ (n = 4), $CuIn_3Se_5$ (n = 5) and $Cu_2In_4Se_7$ (n = 7) etc.[32] As the density of Cu vacancies change, the type of OVC formed (which stabilizes) by traversing n units of $CuInSe_2$ changes keeping free energy (G) of $CuInSe_2$ constant or with negligibly small change. Hence in the free energy schematic (for selenides) with two minima, one corresponding to CISe (remains constant) and the other to OVCs (changes with x). The ΔG which changes with density of Cu vacancies (for OVCs alone) may be small and we do not know the magnitude of ΔG. However, the two minima free energy schematic discussed above should be applicable even if Cu vacancies exhibit ordering over a large range forming OVCs.

Guo *et al.* reported an efficiency of 7.2% under Cu-poor and Zn-rich conditions and 0.23% under stoichiometric

conditions.[19,20] The fundamental mechanism/physics behind the huge increase in the device performance is still a matter of investigation. In the present work, a relation between variation of disorder phonon mode at 331 cm^{-1} with creation of defects by varying Cu stoichiometry and incident laser beam intensity is attributed to basic defect physics associated with Cu based chalcopyrites. Recently, Kosyak *et al*. reported *ab initio* studies on point defects in CZTS where it is reported that defect density influences phonon density of states which in turn affect carrier concentration.[34] In view of the above discussion and the results of the present work, we predict that correlating basic defect physics of material and its influence on phonon spectrum to transport properties may reveal the mechanism behind surge in efficiency under non stoichiometric conditions.

In conclusion, nano-ink based $Cu_{2-x}Zn_{1.3}SnS_4$, thin films for $x = 0$, 0.3, and 0.5 compositions were prepared from nano inks synthesized by adopting an efficient, economic and hydrazine free hot-injection technique and Raman studies were carried out on the thin films. Change in Cu stoichiometry and variation in incident laser beam intensity both induce a disorder in the system giving rise to a disorder phonon mode at 331 cm^{-1} corresponding to PD-KS $(I\bar{4}2m)$ indicing a change over from KS to PD-KS that has effectively the same symmetry as stannite $(I\bar{4}2m)$ which is traced to basic defect physics associated with Cu based chalcopyrites.

The authors thank Department of Science and Technology (DST), New Delhi for facilitating the establishment of "Nano Functional Materials Technology Center" (Grant: SRNM/NAT/02-2005) at IIT Madras. The authors MSR and SKS are thankful for financial help obtained through the DST project (DST/TM/SERI/2K11/111). The author M.K.S. wants to thank CSIR, New Delhi for CSIR-SRF financial support.

[1]J. E. Jaffe and A. Zunger, Phys. Rev. B **64**, 241304 (2001).
[2]C. Persson and A. Zunger, Phys. Rev. Lett. **91**, 266401 (2003).
[3]C. Persson and A. Zunger, Appl. Phys. Lett. **87**, 211904 (2005).
[4]J. B. Li, V. Chawla, and B. M. Clemens, Adv. Mater. **24**, 720 (2012).
[5]T. K. Todorov, J. Tang, S. Bag, O. Gunawan, T. Gokmen, Y. Zhu, and D. B. Mitzi, Adv. Energy Mater. **3**, 34 (2013).
[6]S. Y. Chen, X. G. Gong, A. Walsh, and S. H. Wei, Appl. Phys. Lett. **96**, 021902 (2010).
[7]A. Nagoya, R. Asahi, R. Wahl, and G. Kresse, Phys. Rev. B **81**, 113202 (2010).
[8]D. S. Su, W. Neumann, and M. Giersig, Thin Solid Films **361–362**, 218 (2000).
[9]A. Walsh, S. Y. Chen, S. H. Wei, and X. G. Gong, Adv. Energy Mater. **2**, 400 (2012).
[10]S. Y. Chen, X. G. Gong, A. Walsh, and S. H. Wei, Appl. Phys. Lett. **94**, 041903 (2009).
[11]S. Botti, D. Kammerlander, and M. A. L. Marques, Appl. Phys. Lett. **98**, 241915 (2011).
[12]D. Dumcenco and Y. S. Huang, Opt. Mater. **35**, 419 (2013).
[13]A. Khare, B. Himmetoglu, M. Johnson, D. J. Norris, M. Cococcioni, and E. S. Aydil, J. Appl. Phys. **111**, 083707 (2012).
[14]P. A. Fernandes, P. M. P. Salome, and A. F. da Cunha, J. Alloys Compd. **509**, 7600 (2011).
[15]S. Schorr, Sol. Energy Mater. Sol. Cells **95**, 1482 (2011).
[16]T. Washio, H. Nozaki, T. Fukano, T. Motohiro, K. Jimbo, and H. Katagiri, J. Appl. Phys. **110**, 074511 (2011).
[17]M. Y. Valakh, O. F. Kolomys, S. S. Ponomaryov, V. O. Yukhymchuk, I. S. Babichuk, V. Izquierdo-Roca, E. Saucedo, A. Perez-Rodriguez, J. R. Morante, S. Schorr, and I. V. Bodnar, Phys. Status Solidi R **7**, 258 (2013).
[18]K. Ramasamy, M. A. Malik, and P. O'Brien, Chem. Commun. **48**, 5703 (2012).
[19]Q. Guo, G. M. Ford, W. C. Yang, B. C. Walker, E. A. Stach, H. W. Hillhouse, and R. Agrawal, J. Am. Chem. Soc. **132**, 17384 (2010).
[20]Q. J. Guo, H. W. Hillhouse, and R. Agrawal, J. Am. Chem. Soc. **131**, 11672 (2009).
[21]D. Bhattacharyya, S. Bocking, and M. J. Carter, J. Mater. Sci. **31**, 5451 (1996).
[22]E. Ahmed, M. Amar, W. Ahmed, R. D. Pilkington, A. E. Hill, and M. J. Jackson, J. Mater. Eng. Perform. **15**, 213 (2006).
[23]X. G. Wang, S. S. Li, C. H. Huang, S. Rawal, J. M. Howard, V. Craciun, T. J. Anderson, and O. D. Crisalle, Sol. Energy Mater. Sol. Cells **88**, 65 (2005).
[24]W. C. Liu, B. L. Guo, X. S. Wu, F. M. Zhang, C. L. Mak, and K. H. Wong, J. Mater. Chem. A **1**, 3182 (2013).
[25]M. Grossberg, J. Krustok, J. Raudoja, and T. Raadik, Appl. Phys. Lett. **101**, 102102 (2012).
[26]S. Schorr, M. Tovar, D. Sheptyakov, L. Keller, and G. Geandier, J. Phys. Chem. Solids **66**, 1961 (2005).
[27]D. Huang and C. Persson, Thin Solid Films **535**, 265 (2013).
[28]E. Guneri, F. Gode, B. Boyarbay, and C. Gumus, Mater. Res. Bull. **47**, 3738 (2012).
[29]A. J. Cheng, M. Manno, A. Khare, C. Leighton, S. A. Campbell, and E. S. Aydil, J. Vac. Sci. Technol., A **29**, 051203 (2011).
[30]L. D. Landau and E. M. Lifshitz, *Statistical Physics, Part 1* (Pergamon Press, Oxford, 1980).
[31]H. Yang, L. A. Jauregui, G. Zhang, Y. P. Chen, and Y. Wu, Nano Lett. **12**, 540 (2012).
[32]S. B. Zhang, S.-H. Wei, and A. Zunger, Phys. Rev. Lett. **78**, 4059 (1997).
[33]A. Klein and W. Jaegermann, Appl. Phys. Lett. **74**, 2283 (1999).
[34]V. Kosyak, N. B. M. Amiri, A. V. Postnikov, and M. A. Scarpulla, J. Appl. Phys. **114**, 124501 (2013).